Time-Optimal Control for Circadian Entrainment for a Model with Circadian and Sleep Dynamics

Agung Julius, Jiawei Yin, John T. Wen
Light Enabled Systems and Application (LESA) Engineering Research Center
Rensselaer Polytechnic Institute, Troy, NY

Abstract— **In this paper, we study an optimal control problem for circadian rhythm regulation. The objective of the problem is to find a lighting schedule that minimizes the time required for a subject's circadian rhythm to synchronize with a reference circadian rhythm. We previously solved this problem with a bang-off control algorithm. However, this existing solution neglects the sleep dynamics and often results in an unreasonably uncomfortable schedule (with excessive sleepiness). In this paper, we use a hybrid system model that contains both the circadian and sleep dynamics. Using variational analysis, we show that the time-optimal control problem is still a bang-off control algorithm, but from a class of algorithms that is richer than the one previously reported.**

I. INTRODUCTION

In humans, the circadian rhythm is heavily linked to various physiological processes, including sleep, metabolism, hormone secretion, and neurobehavioral processes. Disruption of the circadian rhythm is known to have negative impacts on health, ranging from fatigue in travelers with jet lag to an increased risk of cancer in rotating shift workers.The sleep process in humans is very tightly connected to the circadian rhythm. The sleep drive, for example, is known to be modulated by the circadian rhythm [1]–[3].

In the literature, there are mathematical models that capture the dynamics of the circadian rhythm and how light affects it. A variety of high-order biochemical models that capture various chemical concentrations in the cells have been reported in [4]–[6]. Empirical models, such as variants of the well-known Kronauer model [7], [8], are simpler and capture the essential behavior of the human core body temperature (CBT) oscillation and the effect of light on the phase and amplitude of this oscillation. As demonstrated in [9], the Kronauer model may be considered as the asymptotic case of the biochemical models in an average sense. In our previous work, we have used a first order phase-reduced model that directly describes the impact of light on the *circadian phase*. We have shown that in solving time-optimal circadian entrainment problem the phase-reduced model is effectively a good approximation of the Kronauer model [10], [11] (also see Fig. 1). There are also models that describe how the dynamics of sleep and neurobehavioral states are coupled to that of the circadian rhythm. The most popular variant, the two-process model, links the dynamics of sleep drive and alertness to the circadian phase [3], [12]. These models can provide quantitative predictions of these processes.

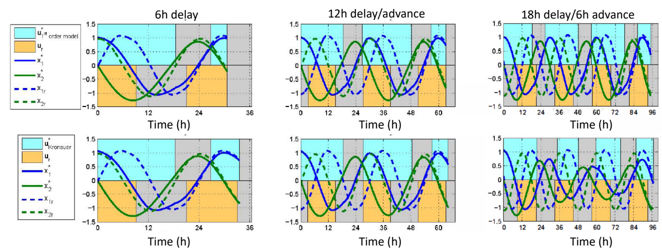

Fig. 1. From [10]. Bang-off solutions of the time-optimal circadian entrainment for various jetlag cases. The top row are the solutions obtained using the first-order phase reduced model. The second row are the solutions obtained using the Kronauer model. The solid and dashed curves represent the circadian phase of the subject and the reference, respectively. Cyan bands represent when the optimal control input (lighting) is on. Orange bands represent when the natural daylight is on (assuming 12h/12h light dark pattern).

Regulation of circadian rhythms is typically expressed as an optimal control problem of a system with nonlinear dynamics. The control inputs into the system are typically light and chemicals such as melatonin. Some researchers have proposed to use model predictive control to deal with the nonlinear dynamics of the circadian rhythm [13]–[15]. Some others consider the time-optimal control problem related to circadian entrainment. Our prior work (c.f. [10], [11], [16], [17]) that used the Pontryagin Minimum Principle approach fall under this category. A related work reported in [18] also posed the time-optimal control problem and solved it using switching time (i.e., between light on and off) optimization. Existing results in the optimal control of circadian rhythms **do not take into account the interplay between the sleep process and the circadian process**. This is apparent, e.g. in the first column of Fig. 1. It shows a scenario where a traveler flies from Paris to NYC and lands at 10 am EST (NYC local time). The optimal lighting schedule dictates that the subject receives (maximum) lighting until approximately 4 am EST the next day! In this paper, we address the time-optimal circadian entrainment problem using the two process model, which also captures the dynamics of sleepiness. Our modeling approach represents the system as a hybrid system with two modes (asleep and awake). We derive the necessary condition for optimality for the light input for this hybrid system based on variational analysis. We further develop an algorithm to compute the optimal control input and demonstrate it on a few representative cases.

II. Modeling Approach and Problem Formulation

A. Two-Process Model for Circadian and Sleep

The sleep homeostasis process $S(t)$, which regulates the sleepiness of the subject is modeled as

$$\frac{dS}{dt} = \begin{cases} -S/\tau_s, & \beta(t) = 1, \\ (1-S)/\tau_a, & \beta(t) = 0. \end{cases} \quad (1)$$

Here, the discrete mode $\beta(t) = 1$ means the subject is asleep, and $\beta(t) = 0$ means the subject is awake. The parameters $\tau_s = 18.2$ h and $\tau_a = 4.2$ h define the time scale of this dynamics.

We choose to use an effective phase-reduced model [10], [11] to describe the dynamics of the circadian rhythm

$$\frac{d\theta}{dt} = \omega_0 + (1-\beta(t))f(\theta)u(t), \quad (2)$$

where θ is the circadian phase in rad. The parameter $\omega_0 = 2\pi/24.2$ rad/h is the so called *free running frequency*. The variable u is the subject's circadian light exposure, which is our control input. The function $f(\theta)$ is called the *phase response function*, given by

$$f(\theta) \triangleq a_0 + \sum_{k=1}^{5} a_k cos(k\theta) + b_k sin(k\theta),$$

with $a_0 = -0.1251, a_1 = 0.02273, b_1 = -0.2844, a_2 = -0.002434, b_2 = 0.1059, a_3 = 0.007844, b_3 = -0.02783, a_4 = -0.001096, b_4 = 0.006338, a_5 = 0.008446$, and $b_5 = -0.003007$.

Sleepiness, $B(t)$, is jointly affected by sleep homeostasis $S(t)$ and the circadian phase $\theta(t)$ through

$$B(t) = S(t) - 0.1333\cos\theta(t). \quad (3)$$

Assumption 1: The switching of the mode $\beta(t)$ is autonomous, and completely characterized by the subject's sleepiness $B(t)$. When $B(t)$ reaches an upper threshold $H_m = 0.67$, the subject spontaneously falls asleep. When $B(t)$ reaches a lower threshold $L_m = 0.17$, the subject wakes up spontaneously. These thresholds are set such that the length of sleep is approximately 8 hours.

Hereafter, equations (1)-(2) and Assumption 1 are collectively referred to as the **system dynamics**.

B. Periodic Solutions under Periodic Inputs: Entrainment

Under the system dynamics and a periodic light input $u(t)$, the state trajectory might also be periodic with the same period. We call this phenomenon *entrainment*. Consider T-periodic inputs that are defined in $[0,T)$ as:

$$u_{\text{ref}}(t) = \begin{cases} u_{\max}, & t \in [0, \alpha T], \\ 0, & t \in [\alpha T, T), \end{cases} \quad (4)$$

where $\alpha \in [0,1]$ is called the *duty-cycle* of the input. The value $u_{\max}$ =0.2392 corresponds to light exposure at 9500 lux.

Based on a numerical study, we found that the existence of a stable entrainment orbit depends on $u_{\max}$, T, and α. Fig. II-B recaps our findings about the existence of stable entrainment orbits.

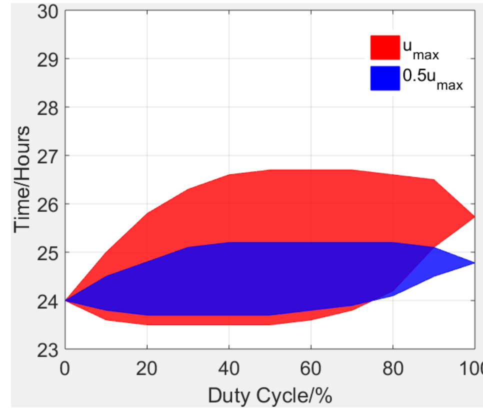

Fig. 2. Values of maximum light intensity, period (T), and duty-cycle (α) for which stable entrainment orbits exist.

In this paper, for circadian entrainment, we focus on a reference trajectory generated using $u_{\text{ref}}(t)$ with T = 24h and α=0.5=50%. This corresponds to a daily routine where light is present between 6 am - 6 pm ($t = 0$ refers to 6 am), and the subject goes to sleep at 11:12 pm and wakes up at 7:18 am.

Notation: Hereafter, we denote the periodic solution of θ and S for $u(t) = u_{\text{ref}}(t)$ with T = 24h and α=50% as $\theta_{\text{ref}}(t)$ and $S_{\text{ref}}(t)$, respectively.

C. Problem Formulation

The time-optimal control problem that we consider in this paper can be formulated as follows.

Problem 2 (Time-Optimal Circadian Entrainment): Given $\theta(0)$ and $S(0)$, find $u(t)$ that minimizes the final time T_f under the constraint of the system dynamics and $\theta(T_f) = \theta_{\text{ref}}(T_f)$.

Note that this problem is different from the ones considered in our earlier work and others in that the sleep dynamics is now a part of the system dynamics.

III. Greedy Strategies and Optimality

We define two greedy (feedback) control strategies, where $u(t)$ is calculated based on $\theta(t)$ as follows:

Greedy Delaying Strategy:

$$u(t) = \begin{cases} u_{\max}, & f(\theta(t)) < 0, \\ 0, & f(\theta(t)) \geq 0. \end{cases} \quad (5)$$

Greedy Advancing Strategy:

$$u(t) = \begin{cases} u_{\max}, & f(\theta(t)) \geq 0, \\ 0, & f(\theta(t)) < 0. \end{cases} \quad (6)$$

We have shown in [11] that *when the sleep dynamics is not considered* (i.e., $\beta(t) \equiv 0$ for the entire entrainment period), then the time-optimal entrainment is achieved using one of the greedy strategies above.

To explain the importance of these two strategies in the problem considered in the current paper, we introduce the following term.

Sleep-wake day. One sleep-wake day is the time interval between two consecutive moments of the subject (spontaneously) waking up.

We can then state the main result of this paper, which will be derived in the next sections.

Main result: The optimal control input for Problem 2 is piecewise greedy. Within each sleep-wake day the optimal control input follows the same greedy strategy (i.e., delaying or advancing) with the possibility of switching greedy strategy after each sleep-wake day.

IV. Optimal Control for Hybrid Systems

Consider a hybrid system with N modes, whose dynamics is given by

$$\text{Mode i: } \dot{x} = F_i(x) + G_i(x)u, \ i \in \{1,2,\cdots,N\}, \tag{7}$$

$x \in \mathbb{R}^n$ and $u \in \mathbb{R}$. We suppose that the system is initialized in Mode 1 at $x(0) = x_0$. The transition between Modes i and $i+1$ occurs at time $t = T_i$ when the state satisfies the switching condition

$$H_i(x(T_i), T_i) = 0. \tag{8}$$

The execution terminates at time $t = T_N$ when, in Mode N, the state satisfies

$$H_N(x(T_N), T_N) = 0. \tag{9}$$

For convenience, we define $T_0 \triangleq 0$. We assume that the functions $H_1, \cdots, H_N$ are smooth and map $\mathbb{R}^n \times \mathbb{R}$ to $\mathbb{R}$. See Fig. 3 for an illustration showing the first 3 modes.

Notation: We denote the control input signal while the system is in Mode i as $u_i(t)$, $x(T_i)$ as x_i, $T_i - T_{i-1}$ as Δ_i, and the solution of the state equation (7) with initial state $x(0) = x_{i-1}$ under input signal $u_i(\cdot)$ as $\xi_i(t; x_{i-1}, u_i)$.

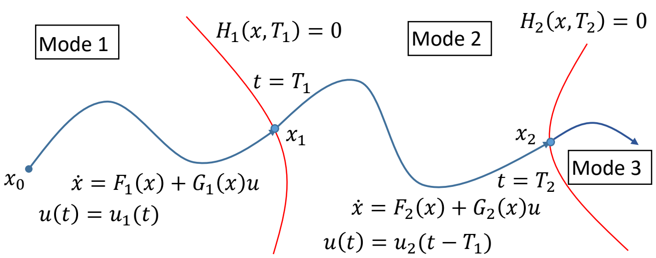

Fig. 3. Illustration of the state trajectories of the hybrid system in Sec. IV

We seek the control input $u(\cdot)$ that minimizes

$$J(u) = T_N = \sum_{i=1}^{N} \Delta_i. \tag{10}$$

We also assume that $u(\cdot)$ is constrained as

$$0 \le u(t) \le u_{\max}, \forall t. \tag{11}$$

A. First Variation Analysis of Δ_i

The constraint (8) can be written as

$$H_i(x_i, T_i) = H_i(\xi_i(\Delta_i; x_{i-1}, u_i), T_i) = 0.$$

Taking the total variation of this equation provides us with the relationship between the variations in x_{i-1} and $u_i(\cdot)$ and the variation in Δ_i.

Notation: We write $\frac{\partial H_i}{\partial x}$ and $\frac{\partial H_i}{\partial T}$ to represent the partial derivatives of H_i with respect to its first and second arguments, respectively.

We then have:

$$\frac{\partial H_i(x_i,T_i)}{\partial x}\left((F_i(x_i)+G_i(x_i)u_i(\Delta_i))\,d\Delta_i + \frac{\partial x_i}{\partial x_{i-1}}dx_{i-1} + \cdots + \frac{\partial x_i}{\partial u_i}du_i\right) + \frac{\partial H_i(x_i,T_i)}{\partial T}d\Delta_i = 0. \tag{12}$$

From (12), assuming that

$$\frac{\partial H_i(x_i,T_i)}{\partial x}(F_i(x_i)+G_i(x_i)u_i(\Delta_i)) + \frac{\partial H_i(x_i,T_i)}{\partial T} \neq 0, \tag{13}$$

we can obtain

$$d\Delta_i = -\frac{\frac{\partial H_i(x_i,T_i)}{\partial x}\left(\frac{\partial x_i}{\partial x_{i-1}}dx_{i-1} + \frac{\partial x_i}{\partial u_i}du_i\right)}{\frac{\partial H_i(x_i,T_i)}{\partial x}(F_i(x_i)+G_i(x_i)u_i(\Delta_i)) + \frac{\partial H_i(x_i,T_i)}{\partial T}}. \tag{14}$$

Note that (13) essentially means that the velocity vector $\dot{x}$ cannot be tangent to the (time-varying) manifold $H_i(x,T) = 0$ at time $t = T_i$, which is the standard transversality condition in optimal control .

In the control theory literature (e.g. [19]), it is known that $\frac{\partial x_i}{\partial x_{i-1}}$ and $\frac{\partial x_i}{\partial u_i}$ can be calculated using the sensitivity function, which we reformulate as the following lemma. Note that this is a corollary of the results given in, e.g., [19], and therefore is presented without proofs.

Lemma 3: We define the transition matrix $\Phi_i(\Delta_i, t) \in \mathbb{R}^{n\times n}$, $t \in [0, \Delta_i]$, as the solution of the time-varying ODE system

$$\frac{d\Phi_i(\Delta_i,t)}{d\tau} = -\Phi_i(\Delta_i,t)\left(\frac{\partial F_i}{\partial x}(\xi_i(t;x_{i-1},u_i)) + \frac{\partial G_i}{\partial x}(\xi_i(t;x_{i-1},u_i))u_i(t)\right), \tag{15}$$

$$\Phi_i(\Delta_i,\Delta_i) = I_{n\times n}. \tag{16}$$

Then,

$$\frac{\partial x_i}{\partial x_{i-1}} = \Phi_i(\Delta_i, 0), \tag{17}$$

$$\frac{\partial x_i}{\partial u_i}(t) = \Phi_i(\Delta_i,t)G_i(\xi_i(t;x_{i-1},u_i)). \tag{18}$$

B. First Variation Analysis of $J(u)$

Because of (10), the first variation of $J(u)$ with respect to u_i can be written as

$$\frac{\partial J}{\partial u_i} = \sum_{k=1}^{N}\frac{\partial \Delta_k}{\partial u_i} = \sum_{k=i}^{N}\frac{\partial \Delta_k}{\partial u_i}. \tag{19}$$

The second equality in (19) is because u_i only affects Δ_k for $k \geq i$. The following lemma recaps how $\frac{\partial \Delta_k}{\partial u_i}$ can be calculated.

Lemma 4:

$$\frac{\partial \Delta_k}{\partial u_i}(t) = \mathfrak{Q}_{k,i}\Phi_i(\Delta_i,t)G_i(\xi_i(t;x_{i-1},u_i), \tag{20}$$

where for $k > i$,

$$\mathfrak{Q}_{k,i} \triangleq -\frac{\frac{\partial H_k(x_k,T_k)}{\partial x}\Phi_k(\Delta_k,0)\Phi_{k-1}(\Delta_{k-1},0)\cdots\Phi_{i+1}(\Delta_{i+1},0)}{\frac{\partial H_k(x_k,T_k)}{\partial x}(F_k(x_k)+G_k(x_k)u_k(\Delta_k))+\frac{\partial H_k(x_k,T_k)}{\partial T}}, \tag{21}$$

and for $k = i$,

$$\mathfrak{Q}_{k,k} \triangleq -\frac{\frac{\partial H_k(x_k,T_k)}{\partial x}}{\frac{\partial H_k(x_k,T_k)}{\partial x}(F_k(x_k)+G_k(x_k)u_k(\Delta_k))+\frac{\partial H_k(x_k,T_k)}{\partial T}}. \tag{22}$$

Therefore, $\frac{\partial J}{\partial u_i}$ can be calculated by combining the use of (19) and (20).

$$\frac{\partial J}{\partial u_i}(t) = \left(\sum_{k=i}^{N}\mathfrak{Q}_{k,i}\right)\Phi_i(\Delta_i,t)G_i(\xi_i(t;x_{i-1},u_i). \tag{23}$$

Notation: For notational simplicity, hereafter we define the $1\times n$ row vector

$$\mathfrak{R}_i(t) \triangleq \left(\sum_{k=i}^{N}\mathfrak{Q}_{k,i}\right)\Phi_i(\Delta_i,t). \tag{24}$$

C. Local Optimality with Respect to Perturbations in $u_i(\cdot)$

The sufficient condition for stationarity of the objective function $J(u)$ with respect to any valid perturbation $\delta u_i(\cdot)$ is obtained from (23):

$$\mathfrak{R}_i(t)G_i(\xi_i(t;x_{i-1},u_i)\cdot\delta u_i(t) \geq 0. \tag{25}$$

Because of the inequality contraints in (11), three different cases emerge for (25) to be true. If $\mathfrak{R}_i(t)G_i(\xi_i(t;x_{i-1},u_i) < 0$, then the optimal input $u_i^*(t) = u_{\max}$. If $\mathfrak{R}_i(t)G_i(\xi_i(t;x_{i-1},u_i) > 0$, then the optimal input $u_i^*(t) = 0$. The case when $\mathfrak{R}_i(t)G_i(\xi_i(t;x_{i-1},u_i) = 0$, implies that any perturbation in $u_i(t)$ does not have first order effect on $J(u)$ and (potentially) leads to a singular arc.

The procedure to calculate $\mathfrak{R}_i(t)$ can be summarized in the following lemma.

Lemma 5: The signal $\mathfrak{R}_i(t)$ for $i\in\{1,\cdots N\}$ and $t\in[0,\Delta_i]$ satisfies the time-varying ODE

$$\frac{d\mathfrak{R}_i(t)}{dt} = -\mathfrak{R}_i(t)\left(\frac{\partial F_i}{\partial x}(\xi_i(t;x_{i-1},u_i))+ \cdots + \frac{\partial G_i}{\partial x}(\xi_i(t;x_{i-1},u_i))u_i(t)\right). \tag{26}$$

Further, the discontinuity from $\mathfrak{R}_i(\Delta_i)$ to $\mathfrak{R}_{i+1}(0)$ is given by

$$\mathfrak{R}_{i+1}(0) = \mathfrak{R}_i(\Delta_i)+\mathfrak{Q}_{i,i}. \tag{27}$$

Remark 1: Because of (22), $\mathfrak{Q}_{i,i}$ in (27) can be calculated based on the instantaneous control input and state at the transition time T_i (when the dynamics switched from Mode i). This feature distinguishes our results from those of, e.g. [20] (specifically Sec. 3.6) and [21] (specifically Eq. (9)). The references above discussed the discontinuity in the co-states at transition times, but did not present explicitly the amount of the discontinuity as we do in (27).

V. Optimal Solutions for the Time-Optimal Circadian Entrainment Problem

We apply the results from the previous section to solve Problem 2. The mode switches at $T_1,\cdots,T_{N-1}$ are the transitions between sleep and awake, and T_N is the time to entrain. Although N cannot be determined a priori, we can derive conditions for the optimal control input, as given in the main result.

Without any loss of generality we can assume that the first mode is an awake mode ($\beta(0) = 0$). Consequently, if we define the states as $x \triangleq [\theta \quad S]^T$, we have for $i \leq N$,

$$F_i\left(\begin{bmatrix}\theta\\ S\end{bmatrix}\right) = \begin{cases}\begin{bmatrix}\omega_0\\ (1-S)/\tau_a\end{bmatrix}, & i \text{ is odd},\\ \begin{bmatrix}0\\ -S/\tau_s\end{bmatrix}, & i \text{ is even}.\end{cases} \tag{28}$$

$$G_i\left(\begin{bmatrix}\theta\\ S\end{bmatrix}\right) = \begin{cases}\begin{bmatrix}f(\theta)\\ 0\end{bmatrix}, & i \text{ is odd},\\ \begin{bmatrix}0\\ 0\end{bmatrix}, & i \text{ is even}.\end{cases} \tag{29}$$

Further, for $i < N$,

$$H_i(x) = \begin{cases} B-0.67 = S-0.1333\cos\theta-0.67, & i \text{ is odd},\\ B-0.17 = S-0.1333\cos\theta-0.17, & i \text{ is even}.\end{cases} \tag{30}$$

The final switching function $H_N(x,T)$ depends explicitly on T as follows:

$$H_N(x) = \theta - \theta_{\text{ref}}(T). \tag{31}$$

When the subject is awake (in odd-numbered modes), we use the results in Sec. IV-C to determine the optimal light input. If we define the notation $\mathfrak{R}_i(t) \triangleq [\mathfrak{R}_i^1(t) \quad \mathfrak{R}_i^2(t)]$, we have

$$u^*(t) = \begin{cases} u_{\max}, & \mathfrak{R}_i^1(t)f(\theta) < 0,\\ 0, & \mathfrak{R}_i^1(t)f(\theta) > 0.\end{cases} \tag{32}$$

Using Lemma 5 (Eq. (26)), we can compute the ODE for $\mathfrak{R}_i(t)$ as follows:

$$\frac{d}{dt}\begin{bmatrix}\mathfrak{R}_i^1(t)\\ \mathfrak{R}_i^2(t)\end{bmatrix} = \begin{bmatrix}-\frac{df(\theta(T_{i-1}+t))}{d\theta}u(T_{i-1}+t)\mathfrak{R}_i^1(t)\\ \frac{1}{\tau_a}\mathfrak{R}_i^2(t)\end{bmatrix}, \tag{33}$$

for odd i, and

$$\frac{d}{dt}\begin{bmatrix}\mathfrak{R}_i^1(t)\\ \mathfrak{R}_i^2(t)\end{bmatrix} = \begin{bmatrix}0\\ \frac{1}{\tau_s}\mathfrak{R}_i^2(t)\end{bmatrix}, \tag{34}$$

for even i. We can observe that $R_i^1(t)$ *does not change its sign within each mode*. This fact and (32) leads to our main result, i.e., *the optimal control strategy in each mode is one of the two greedy strategies*.

Since $\mathfrak{R}_i^1(t)$ is discontinuous at transition times, as given in (27), its sign might change at those times. Hence, *it is possible that the optimal control strategy switches between the two greedy strategies after each sleep-wake day*. Thus, in principle, we need to explore all $2^{N/2}$ possible switching combinations. However, the amount of discontinuity of $\mathfrak{R}_i^1(t)$ as given by (27) and (28) - (30) provides a guideline to narrow the search space. Observe that by those equations, we have

$$\mathfrak{R}_{i+1}^1(0) = \mathfrak{R}_i^1(\Delta_i) - \frac{0.1333\sin\theta(T_i)}{\dot{B}(T_i)}. \tag{35}$$

Therefore, the sign of $\frac{\sin\theta(T_i)}{\dot{B}(T_i)}$ indicates whether it is necessary to consider switching greedy algorithm at transition time T_i as detailed in the following lemma.

Lemma 6: If

$$\operatorname{sign}\left(\mathfrak{R}_i^1(\Delta_i)\right) = -\operatorname{sign}\left(\frac{\sin\theta(T_i)}{\dot{B}(T_i)}\right), \tag{36}$$

then the optimal greedy strategy in Mode $i+1$ is the same as that in Mode i.

Note that it is possible to further sharpen this result by using interval analysis on $\mathfrak{R}_i^1(\Delta_i)$ and $\mathfrak{R}_{i+1}^1(0)$. However, because of space constraint, we do not present this result in the current paper.

VI. Numerical Implementation

To demonstrate the application of our results, we solve Problem 2 for four cases of travelers with jet lag. In each case, we assume that the (time-optimal) circadian entrainment starts as soon as the traveler lands at the destination.

Case 1: A traveler flying from NYC to Paris (6 h advance), landing at ~9 pm local time ($\theta(0) = 0$, $\theta_{\text{ref}}(0) = \pi/2$). Upon arrival, the traveler is not sleepy ($B(0) = 0.17$).

Case 2: Same as Case 1, but the traveler is very sleepy upon arrival ($B(0) = 0.60$).

Case 3: A traveler flying from Paris to NYC (6 h delay), landing at ~9 am local time ($\theta(0) = 0$, $\theta_{\text{ref}}(0) = 3\pi/2$). Upon arrival, the traveler is not sleepy (B(0) = 0.17).

Case 4: Same as Case 3, but the traveler is very sleepy upon arrival (B(0) = 0.60).

The entrainment time of the time-optimal solutions for these cases are 193 h, 220 h, 58 h, and 84 h, respectively. *In each case, we found that the greedy delaying strategy is the optimal control strategy.* We only show the trajectories of the optimal solutions and the reference for Cases 1 and 2 in Fig. 4 because of space limitation.

There are a few points of observation to make based on the results from these 4 cases:

1. It is easier to delay the circadian phase than to advance it. In fact, we showed that it takes less time to achieve 6 h advance by delaying for 18 h. This conclusion is consistent with our previous work that did not consider the sleep dynamics [10], [16], [17].

2. The entrainment times in all four cases are longer than those reported in our earlier work that used the same circadian dynamics but did not consider sleep dynamics and constraint [10] (see Fig. 5). However, if we do not consider the sleep dynamics and constraint, the time-optimal control algorithm results in persistent and excessive sleepiness in the subject.

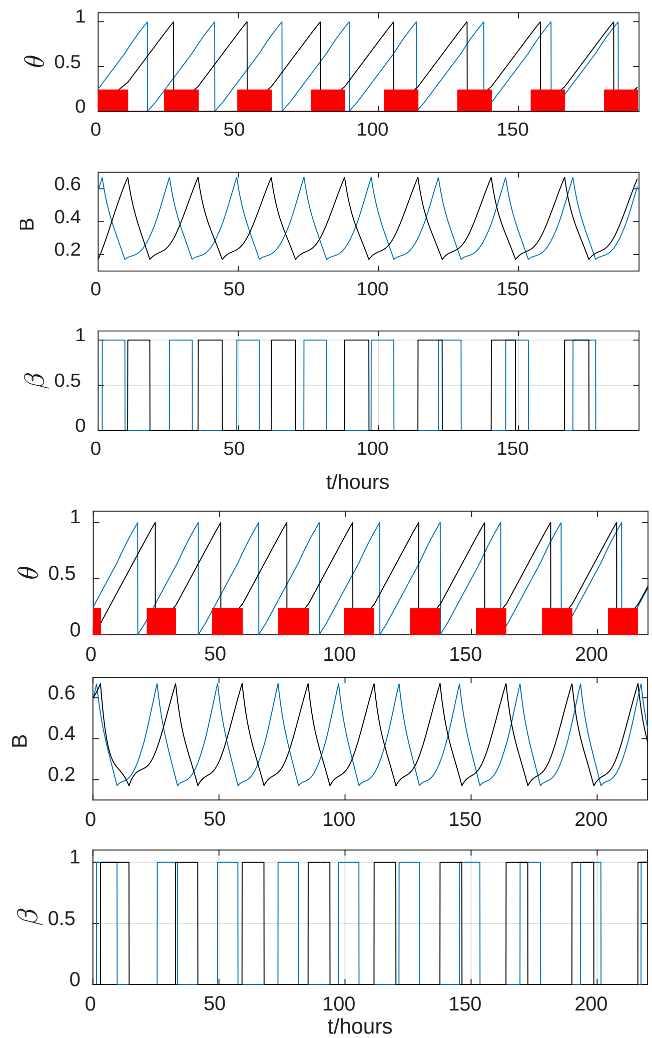

Fig. 4. Time-optimal control solutions for Case 1 (top 3 panels) and Case 2 (bottom 3 panels). The three panels show the circadian phase (in 2π rad), sleepiness, and sleep state (β) of the traveler (black) and the reference (blue). Red pulses represent when the optimal light input is $u_{\max}$.

3. Comparing Case 1 with Case 2, and Case 3 with Case 4, we can see that the initial sleepiness state of the subject significantly influences the optimal solution. One may intuitively guess that the differences in entrainment times in Case 1 vs Case 2 and Case 3 vs Case 4 are approximately the amount of time needed to sleep (~ 8 h). However, it turns out that the differences are actually 26-27 h.

Remark 2: Our model ignores some features found in other papers, such as the Process L. The Process L happens in the retinal photoreceptors and is a precursor to the circadian rhythm dynamics [7], [18]. Nevertheless, preliminary observations suggest that the impact of the Process L in our results is minimal, as shown in Fig. 6.

VII. Conclusions and Future Directions

This paper studies the problem of time-optimal circadian rhythm entrainment using light input. Our paper differs from existing work in this area because we consider the sleep

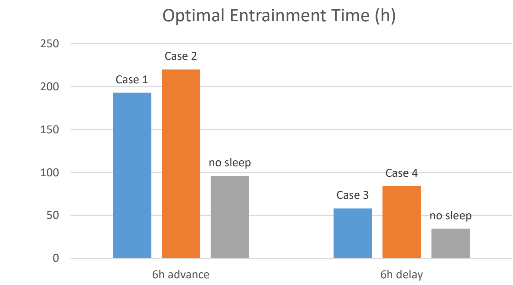

Fig. 5. Comparison of optimal entrainment time for Cases 1 - 4 and the ones without the sleep constraint.

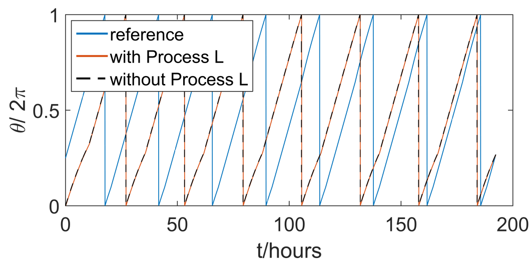

Fig. 6. Comparison between the applications of the time-optimal lighting schedule for Case 1 to the models with and without Process L. The difference is negligible.

dynamics in the problem formulation, and constrain that (a) light input can only be applied when the subject is awake, and (b) the subject sleep-wake schedule is driven by his own sleep dynamics. Our model consists of a hybrid system with two continuous states (1 for the circadian phase, and 1 for the sleep homeostasis), which is consistent with but simpler than the widely accepted Achermann's two-process model. We used variational analysis to derive the main finding of this paper. That is, the optimal control strategy is one of the two greedy strategies that we derived in our earlier work, but with the possibility of switching strategy after each sleep-wake day. The latter was not observed in our previous work.

In the future, we wish to push our research in multiple directions as follows. (1) **More complex models:** Our model ignores aspects of the Kronauer model, such as the Process L and the amplitude of the oscillation. In the future, we will consider the time-optimal circadian entrainment problem for richer models that have these features. (2) **Sleep scheduling:** We currently do not use sleep scheduling as one of the optimization variables. In the future, we can generalize this problem by allowing sleep to be (optimally) scheduled, as long as the schedule does not result in excessive sleepiness. (3) **Optimal feedback control:** We currently solved the time-optimal control problem in a feed-forward fashion. In the future, we will derive optimal feedback control law, e.g., using dynamic programming. Such result will be easier to implement, e.g., in portable smart devices, and potentially more robust against uncertainty and disturbances.

Acknowledgments

This work was supported by the National Science Foundation through the Lighting Enabled Systems and Applications (LESA) ERC (EEC-0812056) and in part by the Army Research Office through a grant entitled "A Quantitative Approach to the Biochronicity of Circadian Rhythm, Sleep, and Neurobehavioral Performance" and by New York State under NYSTAR contract C130145. The authors would like to thank Dr. Wei Qiao for his contribution to the initial portion of this research as part of his postdoctoral research.

References

[1] A. Borbely, "A two process model of sleep regulation," *Human neurobiology*, vol. 1, pp. 195–204, 1982.
[2] S. Daan, D. Beersma, and A. Borbely, "Timing of human sleep: recovery process gated by a circadian pacemaker," *American Journal of Physiology*, vol. 15, pp. R164–R178, 1984.
[3] P. Achermann, "The two-process model of sleep regulation revisited," *Aviation, Space, and Environmental Medicine*, vol. 75, no. 3, pp. A37–A43, March 2004.
[4] J. Baggs, T. Price, L. DiTacchio, S. Panda, G. FitzGerald, and J. Hogenesch, "On discovering low order models in biochemical reaction kinetics," *PLoS Biology*, vol. 7, no. 3, pp. 563–575, Mar. 2009.
[5] J. Leloup and A. Goldbeter, "A model for circadian rhythms in Drosophila incorporating the formation of a complex between the PER and TIM proteins," *Journal of Biological Rhythms*, vol. 13, pp. 70–87, 1998.
[6] J. C. Leloup and A. Goldbeter, "Toward a detailed computational model for the mammalian circadian clock," *Proceedings of National Academy of Science*, vol. 100, pp. 7051–7056, 2003.
[7] D. B. Forger, M. E. Jewett, and R. E. Kronauer, "A simpler model of the human circadian pacemaker," *J. Biological Rhythms*, vol. 14, no. 6, pp. 533–538, 1999.
[8] R. Kronauer, D. Forger, and M. Jewett, "Quantifying human circadian pacemaker response to brief, extended, and repeated light stimuli over the phototopic range," *Journal of Biological Rhythms*, vol. 14, no. 6, pp. 501–516, 1999.
[9] D. Forger and R. Kronauer, "Reconciling mathematical models of biological clocks by averaging on approximate manifolds," *Society for Industrial and Applied Mathematics*, vol. 62, pp. 1281–1296, 2002.
[10] J. Zhang, J. T. Wen, and A. A. Julius, "Optimal and feedback control for light-based circadian entrainment," in *Proc. IEEE Conf. Decision and Control*, 2013, pp. 2677–2682.
[11] W. Qiao, J. T. Wen, and A. A. Julius, "Entrainment control of phase dynamics," *IEEE Trans. Automatic Control*, vol. 62, no. 1, pp. 445–450, 2017.
[12] P. Achermann and A. A. Borbely, "Simulation of daytime vigilance by the additive interaction of a homeostatic and a circadian process," *Biol Cybern*, vol. 71, pp. 115–121, 1994.
[13] C. Mott, D. Mollicone, and M. van Wollen, "Modifying the human circadian pacemaker using model based predictive control," *American Control Conference*, pp. 453–458, 2003.
[14] N. Bagheri, J. Stelling, and F. J. Doyle, "Circadian phase resetting via single and multiple control targets," *PLoS Computational Biology*, pp. 1–10, 2008.
[15] J. H. Abel and F. J. Doyle, "A systems theoretic approach to analysis and control of mammalian circadian dynamics," *Chemical Engineering Research and Design*, vol. 116, pp. 48–69, 2016.
[16] J. X. Zhang, J. T. Wen, and A. A. Julius, "Optimal circadian rhythm control with light input for rapid entrainment and improved vigilance," in *Proc. IEEE Conf. Decision and Control*, 2012, pp. 3007–3012.
[17] J. X. Zhang, W. Qiao, J. T. Wen, and A. A. Julius, "Light-based circadian rhythm control: Entrainment and optimization," *Automatica*, vol. 68, pp. 44–55, 2016.
[18] K. Serkh and D. B. Forger, "Optimal schedules of light exposure for rapidly correcting circadian misalignment," *PLOS Computational Biology*, vol. 10, no. 4, p. e1003523, 2014.
[19] E. D. Sontag, *Mathematical control theory: deterministic finite dimensional systems*, ser. Texts in Applied Mathematics. Springer-Verlag, 1998.
[20] A. E. Bryson and Y. C. Ho, *Applied Optimal Control*. Taylor & Francis, 1975.
[21] M. S. Shaikh and P. E. Caines, "On the hybrid optimal control problem: Theory and algorithms," *IEEE Trans. Automatic Control*, vol. 52, no. 9, pp. 1587–1603, 2007.